MODELLING THE EFFECTS OF RESIDUAL STRESSES ON CLEAVAGE FRACTURE IN WELDED STEEL FRAMES

C. G. Matos and R. H. Dodds, Jr.*

Department of Civil & Environmental Engineering, University of Illinois, Urbana, IL 61801, U.S.A.

ABSTRACT

This study applies an advanced micro-mechanics model of cleavage fracture in ferritic steels to examine the fracture behavior of welded, moment resistant steel frames of the type widely constructed prior to the Northridge earthquake. The Weibull stress model for cleavage, coupled with 3-D analyses of connections containing crack-like defects, provides a quantitative estimate of the cumulative failure probabilities with increasing beam moment. The 3-D models incorporate the complex geometry of a typical welded joint. A set of previously conducted, 15 full-scale tests on T–connections of the pre-Northridge design provide fracture moments to calibrate parameters of the Weibull stress model. Once calibrated, the model is used to examine the importance of welding induced residual stresses in the lower-flange. The model predicts the cumulative failure probability as a function of beam moment.

Keywords: Residual stresses, Cleavage, Eigenstrain, Northridge earthquake

1. INTRODUCTION

Fractures in the connections of welded steel moment resistant frames (WSMFs) during the 1994 Northridge earthquake prompted new research efforts to understand the causes and to develop improved designs [1]. WSMFs constructed prior to the Northridge event often have large rolled sections of A36 (beams) and A572 (columns) steels with flux-core field welds to connect the beam flanges with the column face (see Fig. 1). The geometry of the connection includes an access hole in the beam web, backup bars left in-place, bolted shear tabs, continuity plates in the columns at the beam flange locations, etc. Post-quake field surveys and laboratory tests of full-scale connections indicate the existence of relatively long, shallow defects in the lower-flange weld [2,3]. Fractures initiate at this location and propagate in a very rapid, brittle mode possibly preceded by a small amount of stable ductile tearing ($\lesssim$1–2 mm) [4]. The full-scale connection tests often exhibit limited macroscopic plastic deformation as measured by the plastic rotation (θ_p) prior to the brittle fracture event [5].

This work focuses on understanding and characterizing the brittle fracture behavior for the existing inventory WSMFs having the pre-Northridge design. The approach combines a probabilistic, micro-mechanical model to describe the cleavage fracture process with large-scale, 3-D finite element analyses of the full connections to compute the crack-front stress fields that capture local variations of the fracture parameters and constraint. Applications of this analysis capability examine the relative importance of welding induced residual stresses on the probability for cleavage fracture initiation at the interface of the beam flange and column face.

2. STATISTICAL ANALYSIS OF FULL JOINT TESTS

The tests of pre-Northridge style connections [5] define a set of fifteen specimens having very similar construction. Each of the fifteen specimens reportedly failed in a brittle fracture mode, with fracture initiating in the lower-flange beam-to-column weld. The individual test reports include overall specimen geometry and the measured load at fracture, *P*. This information enables computation of a nominal fracture moment, M_f, at the location where the lower-flange weld connects to the adjacent column flange. Despite the nominal specification of A36 steel for the beams, measured yield strengths from beam flange coupons varied widely. To accommodate the variations in beam sizes and yield strengths in the statistical analysis, fracture moments are normalized by the plastic moment of the section

$$\frac{M_f}{M_P} = \frac{P\ell}{Z\sigma_{ys}} \tag{1}$$

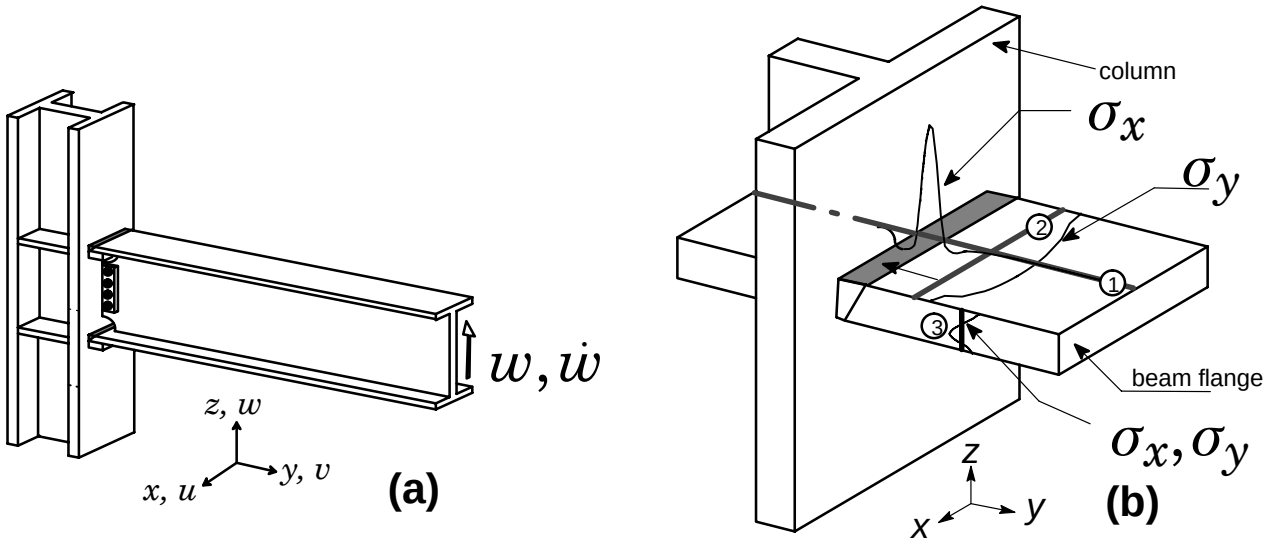

Fig. 1. (a) Schematic of typical pre-Northridge beam-column connection. (b) Typical patterns of residual stresses

where ℓ denotes the reported distance from the centerline of the load actuator to the column face, σ_{ys} defines the reported (coupon) yield stress of the beam flange for each test specimen and *Z* denotes the plastic modulus of the beam cross section. The very strong similarity of geometry and fabrication in these test specimens leads to the postulate that the large variation in values for the normalized fracture moment arises from the expected statistical scatter of toughness values for cleavage fracture in the ductile-to-brittle transition (DBT) region (combined with observed scatter of flaw sizes). Median estimates for the rank failure probability of normalized fracture moment, M_f/M_P, are given by $\mathcal{P}_f = (j - 0.3)/(n + 0.4)$, where *j* denotes the rank (failure) order by increasing M_f/M_P and *n* denotes the sample size (in this case $n = 15$). Normalized values of fracture moment should follow a Weibull distribution as do toughness values for cleavage fracture [6]. The simple, two-parameter Weibull distribution for the cumulative failure probability (median rank) has the form described in Fig. 2a.

3. THE WEIBULL STRESS MODEL

In the DBT region of ferritic steels, the cumulative failure probability follows a three-parameter Weibull distribution in terms of the Weibull stress [7]),

$$P_f(\sigma_w) = 1 - \exp\left[- \left(\frac{\sigma_w - \sigma_{w-\min}}{\sigma_u - \sigma_{w-\min}} \right)^m \right]. \tag{2}$$

where σ_w represents the Weibull stress defined as the integral of a weighted value of the maximum principal (tensile) stress (σ_1) over the process zone of cleavage fracture (i.e., the crack front plastic zone),

$$\sigma_w = \left[\frac{1}{V_0} \int_{\overline{V}} \sigma_1^m dV \right]^{1/m} \tag{3}$$

where $\overline{V}$ represents the volume of the cleavage fracture process zone and *m* denotes the Weibull modulus which defines the shape of the probability density function for microcrack size in the fracture process zone. The parameters σ_u and $\sigma_{w-\min}$ appearing in Eq. (2) denote the scale parameter of the Weibull distribution and the threshold σ_w-value for cleavage fracture respectively. Cleavage fracture cannot occur if $\sigma_w < \sigma_{w-\min}$. Under SSY conditions, $\sigma_{w-\min}$ is σ_w for an experimentally estimated value of $K_{I-\min} \approx 20$ MPa$\sqrt{\text{m}}$ for common ferritic steels..

4. NUMERICAL PROCEDURES

4.1. Modeling of Residual Stresses

The eigenstrain approach [11] used here proves especially convenient to introduce residual stresses in 3-D finite element models. Matos and Dodds [12] developed a field of eigenstrains to generate residual stresses in single-V

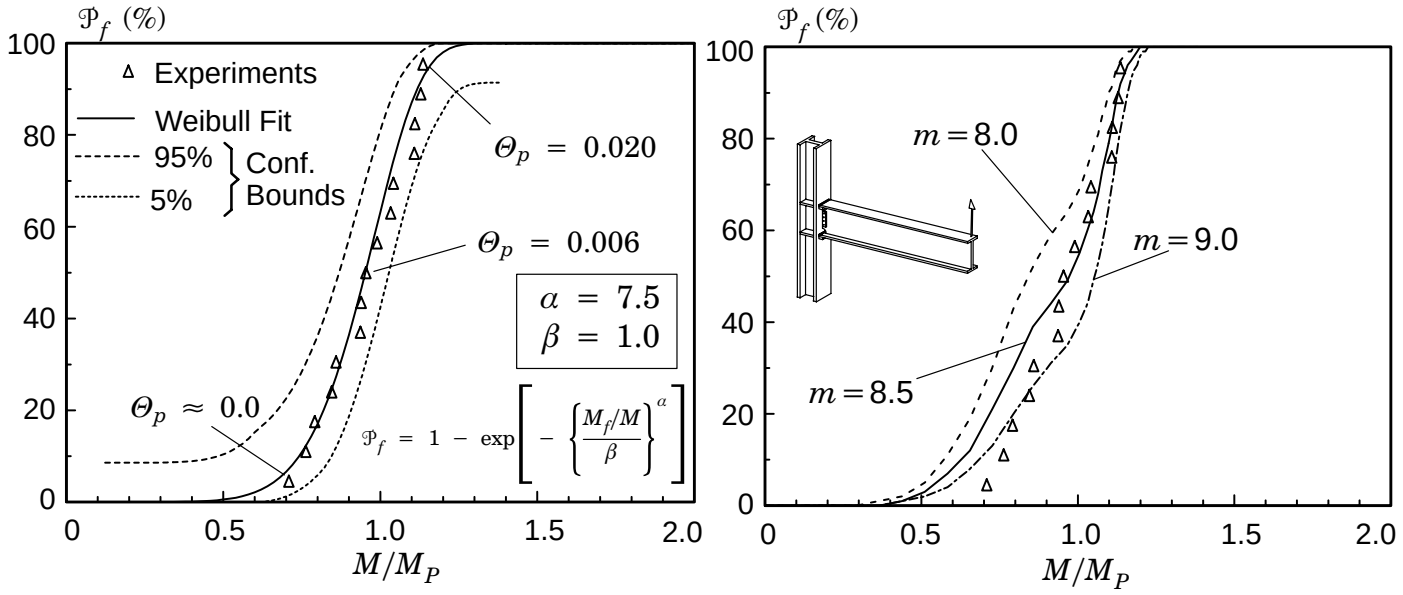

Fig. 2. (a) Weibull fit of experimental tests. (b) Weibull stress calibration of full-joint connections.

groove welds used to join the lower beam flange to the column flange. The residual stress field generated by these eigenstrain functions closely matches the field computed using thermomechanical simulation of a multi-pass welding process for this configuration [13]. Figure 1b depicts key features of this residual stress field. The weld longitudinal stresses (σ_{xx}) along line 1 reach values of the weld metal yield stress (σ_{ys}^{wm}) but decay rapidly to zero outside the weld. Weld transverse stresses (σ_{yy}) along line 2 have a smaller magnitude. Distributions of σ_{xx} and σ_{yy} over the beam flange thickness (along line 3) have tensile stresses at the surfaces and compression at the center. The eigenstrain functions to generate these residual stresses have the form:

$$\epsilon_{ij}^{*} = -\frac{\sigma^{*}}{E} f_{ij}(x,y,z) \tag{4}$$

where $\sigma^{*} = \sigma_{ys}^{wm}$ scales the stress amplitudes defined by the normalized functions $f_{ij}(x,y,z)$. A unit temperature change coupled with anisotropic thermal expansion coefficients, α_{ij}, equal to the ϵ_{ij}^{*} values sampled at element centers provides a simple mechanism to introduce these eigenstrains into the computational model [12].

4.2. Specimen Configurations and Materials

The finite element analyses of the full connection use a non-AISC standard section for the beam with depth $d = 762$ mm, flange width $b_f = 152$ mm, web thickness $t_w = 13$ mm, and flange thickness $t_f = 25$ mm. The column corresponds to a W14 × 176 section. Inspections of welded connections in buildings and in full-scale joints fabricated under laboratory conditions [2] reveal a range of crack-like defects along the root pass of the welds. Lack-of-fusion type defects of variable depth can extend the full width of the weld. These observations led to the adoption in this study of a uniform depth, sharp crack that extends the full width of the beam flange. The crack "depth" equals the applicable backup bar dimension (9.5 or 3.2 mm), plus an additional $a_0 = 5.7$ mm to reflect a typical bead size for the weld root pass. Symmetry of the geometry and loading permits modeling of only one-half of the specimen. The mesh has 34 focused rings of elements in the radial direction surrounding the crack front and 20 elements along the crack front length (half of the beam flange width). The crack tip has a small, initial radius of 20 μm to enhance convergence of the finite-strain solutions.

Stress-strain curves for quasi-static loading rates are constructed from the engineering strain-stress curves reported by Kaufmann *et al.* [17]. The finite element analyses thus have three different materials (beam A36, column A572 and weld metal E70T-4).

4.3. Loading and Boundary Conditions

The loading protocol for quasi-static analyses follows this sequence: 1. Apply the eigenstrains to introduce residual stresses through a total temperature increase of 1°. The temperature increase acts with specified anisotropic thermal expansion coefficients for each element in the weld region to generate the eigenstrains. Use ten, uniform increments of 0.1° to resolve the small amount of resulting plastic deformation. 2. Increase the beam tip

deflection monotonically (quasi-static) through 500 variably sized increments to reach a maximum tip deflection of 254 mm.

4.4. Finite Element Models

Models for fracture analyses are constructed using three-dimensional, 8-node elements with $\overline{B}$ formulation. *J*-integral values are evaluated with a domain integral procedure [14] using domains defined outside the material having non-proportional strain histories at the crack front. The computed *J*-values reflect finite strain effects and thermal strains used to produce the residual stresses. With the inclusion of additional terms that arise from the anisotropic thermal expansion coefficients to model the eigenstrains [12], the *J*-values maintain a strong path independence. The WARP3D [15] code supports computation of crack front average *J*-values and pointwise *J*-values at each node location along the crack front.

5. RESULTS AND DISCUSSION

5.1. Calibration of Weibull Stress Parameters

A two-parameter Weibull distribution, with moments normalized by the beam plastic moment, describes very well the measured distribution of fracture moments in the 15 nearly identical tests conducted on the pre-Northridge design (A36 beams, A572 columns, E70T-4 welds). Fig.2a shows the fit of $\mathcal{P}_f = 1 - exp(-\left\{(M/M_f)/\beta\right\}^{\alpha})$ where the the Weibull modulus is 7.5 with a scale factor of 1.0. The most ductile of the 15 tests reached a total (joint) plastic rotation (Θ_p) of 0.021 radians [16]. Post-processing of the 3-D, nonlinear finite element analyses (including residual stresses) to compute the evolution of Weibull stress values with beam moments at the column face enables calibration of parameters for the recently modified Weibull stress model: $m = 8.5$, $\sigma_u = 2.4\sigma_{ys}$, and $\sigma_{w-\min} = 1.25\sigma_{ys}$. Fig. 2b shows the calibrated Weibull distribution from the finite element analyses which lies well within the 90% confidence bounds for the experimental data. Other curves illustrate the strong sensitivity to the fit value of *m*.

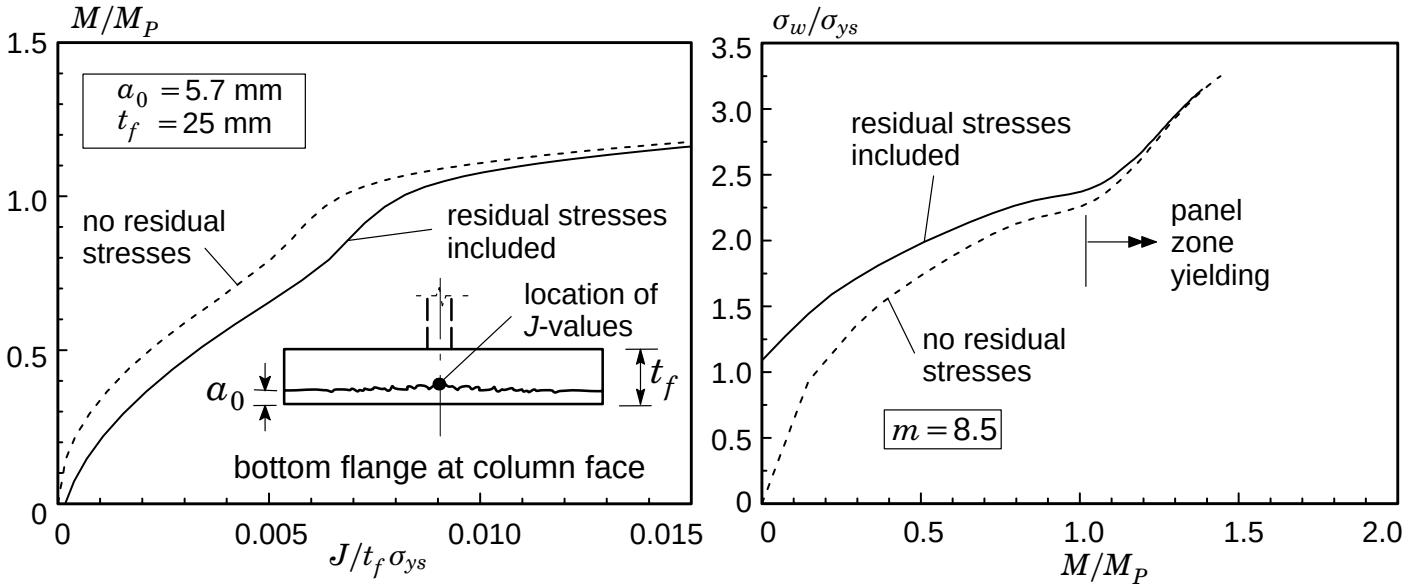

Fig. 3. (a) Development of *J* at center of beam flange. (b) Weibull stress vs. moment at the column face.

5.2. Effects of Residual Stresses: Pre-Northridge Connection

Figure 3a quantifies the impact of residual stresses on the development of *J*-values under increased moment at the column face. These locally computed *J*-values refer to the center of the beam flange as indicated on the figure, where the largest values occur across the full-width of the crack. Early in the loading, the residual stresses increase *J*-values by approximately 20% or equivalently about 15 MPa$\sqrt{m}$ in terms of the stress intensity factor. This essentially fixed increment of crack front loading remains effective throughout but decreases in relative magnitude as the total *J*-values increase rapidly once the connection progresses toward formation of a plastic

hinge. Figure 3b shows a similar influence of residual stresses on the Weibull stress. The strong upswing in σ_w values at $M/M_P \approx 1$ for both curves corresponds to the onset of panel zone yielding in the column. The relatively large σ_w values early in the loading caused by the residual stresses indicate a substantially larger probability for cleavage fracture. Again, once the plastic deformation leads to increased σ_w values later in the loading, the relative importance of the residual stress effect diminishes rapidly. These observations agree with the conventional tenet that residual stress effects decrease in significance under large scale yielding.

Figure 4 shows the effects of residual stresses on the probability of cleavage fracture with moment at the column face as the loading parameter. The residual stresses increase the crack front constraint slightly (in terms of the Weibull stress) for M/M_P values < 0.6. When inserted in the Weibull stress model and combined with the applied load, residual stresses increase the (absolute) cumulative fracture probabilities by 10% for M/M_P values < 0.75, and by 20% for M/M_P values > 0.9.

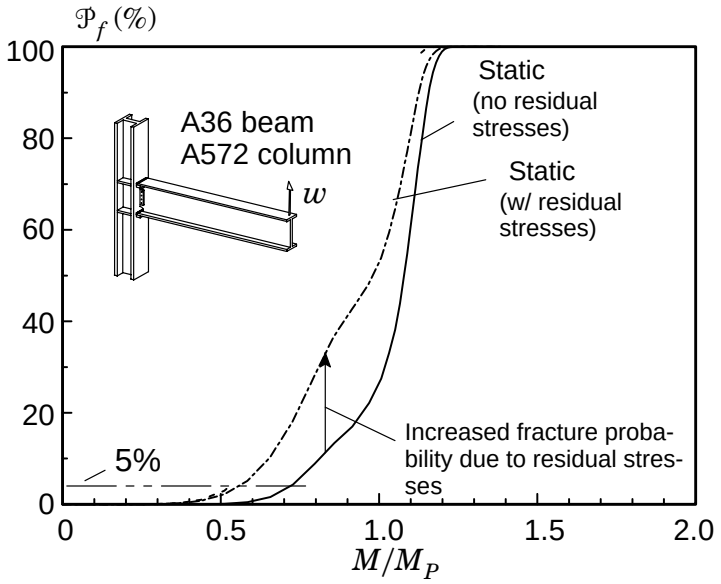

Fig. 4. Cumulative failure probabilities predicted by Weibull stress model.

6. CONCLUDING REMARKS

This study describes probabilistic modeling of the nonlinear fracture behavior in the beam lower-flange to column welds found in moment resistant frames of the design commonly used prior to the Northridge earthquake. 3-D finite element analyses, coupled with an advanced micro-mechanical fracture model based on the Weibull stress, are used to assess the relative significance of residual stresses. The present work considers only the initiation of *brittle fracture* triggered by a *transgranular cleavage* mechanism typical of that exhibited by ferritic steels (and welds) operating in the DBT region.

The finite element models represent the commonly used T-configuration tested in laboratories to simulate exterior connections. Loading takes place through specified displacements imposed at the end of the beam. A realistic residual stress field is introduced using an eigenstrain approach. Measured fracture loads from 15 earlier tests conducted as part of the SAC-Steel and other programs on nearly identical, full-scale T-connections of the pre-Northridge design provide a statistically significant data set to enable calibration of the micro-mechanical model. The computational studies here focus on comparison of the various configurations through the cumulative failure probabilities predicted by the Weibull stress model with loading expressed in terms of the normalized beam moment at the column flange.

REFERENCES

[1] The SAC Joint Venture is a partnership of the Structural Engineers Association of California, the Applied Technology Council, and the California State Universities for Earthquake Engineering.

[2] Kauffmann E. J., Fisher J. *Fracture analysis of failed moment frame weld joints produced in full-scale laboratory tests and buildings damaged in the Northridge earthquake. SAC* 95-08, part 2, 1996;1-1 – 1-21.

[3] Interim Guidelines: *Evaluation, Repair, Modification and Design of Welded Steel Moment Frame Structures*. FEMA-267, Federal Emergency Management Agency, 1995.

[4] Barson J., Pellegrino J. *Failure analysis of welded steel moment–resisting frame connections.* Part II*: pre–Northridge welded steel moment frame connections.* SAC/BD–99/23,2000.

[5] Connection Test Summaries. *Program to reduce the earthquake hazards of steel moment frame structures.* FEMA-289, 1997.

[6] Beremin FM. *A local criterion for cleavage fracture of a nuclear pressure vessel steel. Metall. Trans.* 1983;11:2277-2287.

[7] Gao X, Dodds R. H. Jr. *A Weibull stress model to predict cleavage fracture in plates containing surface cracks. Fatigue & Fracture of Engineering Materials and Structures* 1999;22:481–493.

[8] Gao X, Dodds R. H., Tregoning RL, Joyce JA. *Effects of loading rate on the Weibull stress model for simulation of cleavage fracture in ferritic steels.* Submitted to *Fatigue Fracture Engng Mater Struct* 2000.

[9] Minami F., Ochiai T., Kubo T., Shimanuki H, Arimochi K, *Evaluation of pre-straining and dynamic loading effects on fracture toughness of structural steels by the local approach.* ASME 2000; *PVP Conference*.

[10] Minami F., Ochiai T., Hashida T., Arimochi K, Konda N. *Local approach to dynamics fracture toughness evaluation*. To appear in *ASTM STP* 31st National symposium on *Fatigue and Fracture Mechanics*, 2001.

[11] Mura T. *Micromechanics of Defects in Solids.* Kluwer Academy Publishers. The Netherlands, 1991.

[12] Matos C. G., Dodds R.H. Jr. *Modeling the effects of residual stresses on defects in welds of steel frame connections. Engng Struct* 2000;22:1103–1120.

[13] Zhang J., Dong P. *Residual stresses in welded moment frames and implications on structural performance. J Struct Engng* 2000;126:306–315.

[14] Moran B., Shih C..F. *A general treatment of crack tip contour integrals. International Journal of Fracture* 1987; 35:295-310.

[15] Koppenhoefer K., Gullerud A., Ruggieri C, Dodds R, Healy B. *WARP3D. Structural Research Series* (SRS) 596, UILU-ENG-94-2017, University of Illinois at Urbana-Champaign, 1998.

[16] Matos C. G., Dodds R. H. *Probabilistic fracture modeling of welds in steel frame connections.* Part I*: Quasi-static loading.* Engng Struct, 2000 (in press).

[17] Ricles J, Mao C, Kaufmann E, Lu L, Fisher J. *Dynamic tension test of simulated welded beam flange connection.* SAC Task 7.05, Preliminary Report, 1999.